



Humans incorporate attention-dependent uncertainty into perceptual decisions and confidence

Rachel N. Denison^{a,b,1,2}, William T. Adler^{b,1}, Marisa Carrasco^{a,b}, and Wei Ji Ma^{a,b}

^aDepartment of Psychology, New York University, New York, NY 10003; and ^bCenter for Neural Science, New York University, New York, NY 10003

Edited by Barbara Anne Doshier, University of California, Irvine, CA, and approved September 6, 2018 (received for review October 11, 2017)

Perceptual decisions are better when they take uncertainty into account. Uncertainty arises not only from the properties of sensory input but also from cognitive sources, such as different levels of attention. However, it is unknown whether humans appropriately adjust for such cognitive sources of uncertainty during perceptual decision-making. Here we show that, in a task in which uncertainty is relevant for performance, human categorization and confidence decisions take into account uncertainty related to attention. We manipulated uncertainty in an orientation categorization task from trial to trial using only an attentional cue. The categorization task was designed to disambiguate decision rules that did or did not depend on attention. Using formal model comparison to evaluate decision behavior, we found that category and confidence decision boundaries shifted as a function of attention in an approximately Bayesian fashion. This means that the observer's attentional state on each trial contributed probabilistically to the decision computation. This responsiveness of an observer's decisions to attention-dependent uncertainty should improve perceptual decisions in natural vision, in which attention is unevenly distributed across a scene.

attention | perceptual decision | confidence | Bayesian | criterion

Sensory representations are inherently noisy. In vision, stimulus factors such as low contrast, blur, and visual noise can increase an observer's uncertainty about a visual stimulus. Optimal perceptual decision-making requires taking into account both the sensory measurements and their associated uncertainty (1). When driving on a foggy day, for example, you may be more uncertain about the distance between your car and the car in front of you than you would be on a clear day and try to keep further back. Humans often respond to sensory uncertainty in this way (2, 3), adjusting their choice (4) behavior as well as their confidence (5). Confidence is a metacognitive measure that reflects the observer's degree of certainty about a perceptual decision (6, 7).

Uncertainty arises not only from the external world but also from one's internal state. Attention is a key internal state variable that governs the uncertainty of visual representations (8, 9); it modulates basic perceptual properties like contrast sensitivity (10, 11) and spatial resolution (12). Surprisingly, it has been suggested that, unlike for external sources of uncertainty, people fail to take attention into account during perceptual decision-making (13–15), leading to inaccurate decisions and overconfidence—a risk in attentionally demanding situations like driving a car.

However, this proposal has never been tested using a perceptual task designed to distinguish fixed from flexible decision rules, nor has it been subjected to formal model comparison. Critically, as we show in *SI Appendix, section S1*, the standard signal detection tasks used previously cannot, in principle, test the fixed decision rule proposal. In standard tasks, the absolute internal decision rule cannot be uniquely recovered, making it impossible to distinguish between fixed and flexible decision rules (*SI Appendix, Fig. S1A*).

Testing whether observers take attention-dependent uncertainty into account for both choice and confidence also requires a task in which such decision flexibility stands to improve categorization performance. This condition is not met by traditional left versus right categorization tasks, in which the optimal choice boundary is the same (halfway between the means of the left and right category distributions) regardless of the level of uncertainty (*SI Appendix, Fig. S1B*). Optimal performance can be achieved simply by taking the difference between the evidence for left and the evidence for right, with no need to take uncertainty into account. The same principle applies to present versus absent detection tasks.

To overcome these limitations, we used a categorization task—which we call the embedded category task—specifically designed to test whether decision rules depend on uncertainty. Observers categorized stimuli as belonging to one of two distributions, which had the same mean but different variances (Fig. 14). The task requires distinguishing a more specific from a more general perceptual category (4, 5), which is typical of object recognition (16, 17) (e.g., distinguishing a beagle from other dogs) and perceptual grouping (e.g., distinguishing collinear line segments from other line segment configurations) (18). In the embedded category task, the optimal choice boundaries shift as uncertainty increases, which allowed us to determine whether observers' behavior tracked these shifts, along with analogous shifts in confidence boundaries.

Significance

We must routinely make decisions based on uncertain sensory information. Sometimes that uncertainty is related to our own cognitive state, such as when we are not paying attention. Do our decisions about what we perceive take into account our attentional state? Or are we blind to such internal sources of uncertainty, leading to poor decisions and overconfidence? We found that human observers take attention-dependent uncertainty into account when categorizing visual stimuli and reporting their confidence in a task in which uncertainty is relevant for performance. Moreover, they do so in an approximately Bayesian fashion. Human perceptual decision-making can therefore, at least in some cases, adjust in a statistically appropriate way to external and internal sources of uncertainty.

Author contributions: R.N.D., W.T.A., M.C., and W.J.M. designed research; R.N.D. and W.T.A. performed research; R.N.D. and W.T.A. analyzed data; and R.N.D., W.T.A., M.C., and W.J.M. wrote the paper.

The authors declare no conflict of interest.

This article is a PNAS Direct Submission.

Published under the [PNAS license](#).

Data deposition: All data and code used for running experiments, model fitting, and plotting are available at <https://doi.org/10.5281/zenodo.1422804>.

¹R.N.D. and W.T.A. contributed equally to this work.

²To whom correspondence should be addressed. Email: rachel.denison@nyu.edu.

This article contains supporting information online at www.pnas.org/lookup/suppl/doi:10.1073/pnas.1717720115/-DCSupplemental.

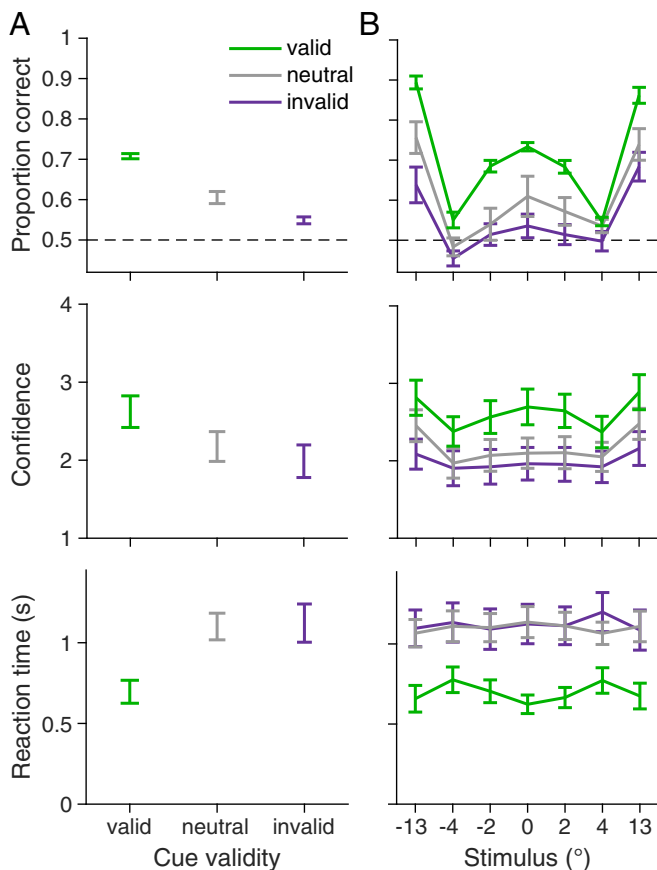


Fig. 2. Behavioral data. $n = 12$ observers. Error bars show trial-weighted mean and SEM across observers. (A) Accuracy, confidence ratings, and reaction time as a function of cue validity. (B) As in A but as a function of cue validity and stimulus orientation. Stimulus orientation is binned to approximately equate the number of trials per bin. *SI Appendix, Fig. S5* shows proportion category 1 choice data, and *SI Appendix, Fig. S6* shows confidence and reaction time data in more detail.

Although our main question was whether observers' decisions took uncertainty into account, our methods also allowed us to determine whether Bayesian computations were necessary to produce the behavioral data or whether heuristic strategies of accounting for uncertainty would suffice. We tested two models with heuristic decision rules in which the decision boundaries vary as linear or quadratic functions of uncertainty, approximating the Bayesian boundaries (*SI Appendix, Fig. S3A*). The Linear and Quadratic models both outperformed the Fixed model (LOO differences of 124 [77, 177] and 129 [65, 198], respectively; *SI Appendix, Fig. S3 B and C*). The best model, quantitatively, was Quadratic, similar to previous findings with contrast-dependent uncertainty (4, 5). *SI Appendix, Table S2* shows all pairwise comparisons of the models. Model recovery showed that our models were meaningfully distinguishable (*SI Appendix, Fig. S4*). Decision rules therefore changed with attention without requiring Bayesian computations.

We next asked whether category decision boundaries—regardless of confidence—shift to account for attention-dependent uncertainty. Perhaps, for example, performance of the Bayesian model was superior not because observers changed their categorization behavior but because they rated their confidence based on the attention condition, which they knew explicitly. Given the mixed findings on the relation between attention and confidence (30–33) and the proposal that perceptual decisions do not account for attention (13), such a finding would not be trivial

(see *Discussion*), but it would warrant a different interpretation than if category decision boundaries also depended on attention. We fit the four models to the category choice data only and

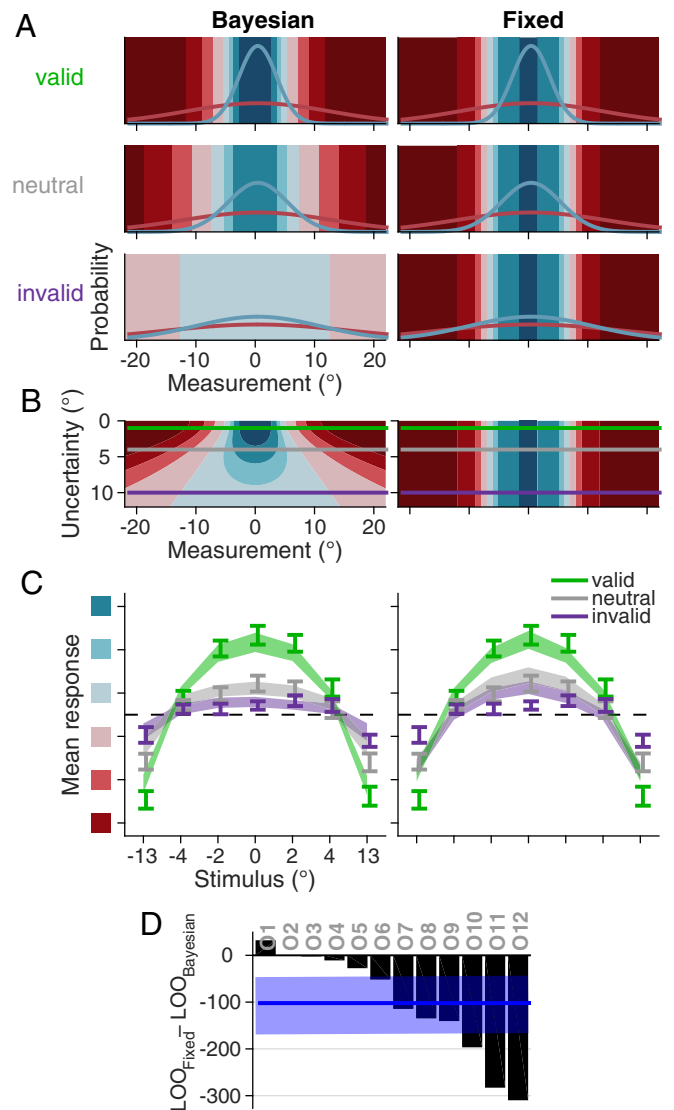


Fig. 3. Model schematics, fits, and fit comparison. (A) Schematic of Bayesian (Left) and Fixed (Right) models, which were fit separately for each observer. As attention decreases, uncertainty (measurement noise SD) increases, and orientation measurement likelihoods (blue and red curves) widen (28). In the Bayesian model, choice and confidence boundaries change as a function of uncertainty. In the Fixed model, boundaries do not depend on uncertainty. Colors indicate category and confidence response (color code in Fig. 1B). (B) Decision rules for Bayesian and Fixed models show the mappings from orientation measurement and uncertainty to category and confidence responses. Horizontal lines indicate the uncertainty levels used in A; the regions intersecting with a horizontal line match the regions in the corresponding plot in A. (C) Model fits to response as a function of orientation and cue validity. Response is an 8-point scale ranging from high confidence category 1 to high confidence category 2, with colors corresponding to those in Fig. 1B; only the middle six responses are shown. Error bars show mean and SEM across observers. Shaded regions are mean and SEM of model fits (see *SI Appendix, section S3.8*). Although mean response is shown here, models were fit to raw, trial-to-trial data. Stimulus orientation is binned to approximately equate the number of trials per bin. (D) Model comparison. Black bars represent individual observer LOO differences of Bayesian from Fixed. Negative values indicate that Bayesian had a higher (better) LOO score than Fixed. Blue line and shaded region show median and 95% confidence interval (CI) of bootstrapped mean differences across observers.

again rejected the Fixed model (*SI Appendix, Fig. S5 A and B and Tables S3 and S4*). Therefore, category criteria, independent of confidence criteria, varied as a function of attention-dependent uncertainty.

Finally, we directly tested for decision boundary shifts—the key difference between the Bayesian and Fixed models—by estimating each observer’s category decision boundaries non-parametrically. To do so, we fit the category choice data with a Free model in which the category decision boundaries varied freely and independently for each attention condition. The estimated boundaries differed between valid and invalid trials (Fig. 4 and *SI Appendix, Fig. S5C*), with a mean difference of 7.5° ($SD = 7.8^\circ$), two-tailed paired t test, $t(11) = 3.33$, $P < 10^{-2}$. Most observers showed a systematic outward shift of category decision boundaries from valid to neutral to invalid conditions, confirming that their choices accounted for uncertainty.

Discussion

Using an embedded category task designed to distinguish fixed from flexible decision rules, we found that human perceptual decision-making takes into account uncertainty due to spatial attention, when uncertainty is relevant for performance. These findings indicate flexible decision behavior that is responsive to attention—an internal factor that affects the uncertainty of stimulus representations.

Our findings of flexible decision boundaries run counter to a previous proposal that observers use a fixed decision rule under varying attentional conditions (13–15, 21). This idea originated from a more general “unified criterion” proposal (25, 26), which asserts that in a display with multiple stimuli, observers adopt a single, fixed decision boundary (the unified criterion) for all items (22–27). The unified criterion proposal implies a rigid, sub-optimal mechanism for perceptual decision-making in real-world complex scenes, in which uncertainty can vary due to a variety of factors.

Although the unified criterion proposal has served to explain experimental findings (13–15, 21–27, 34), it is impossible to infer decision boundaries from behavior in the signal detection theory (SDT) tasks used previously (35). In theory, it is always possible

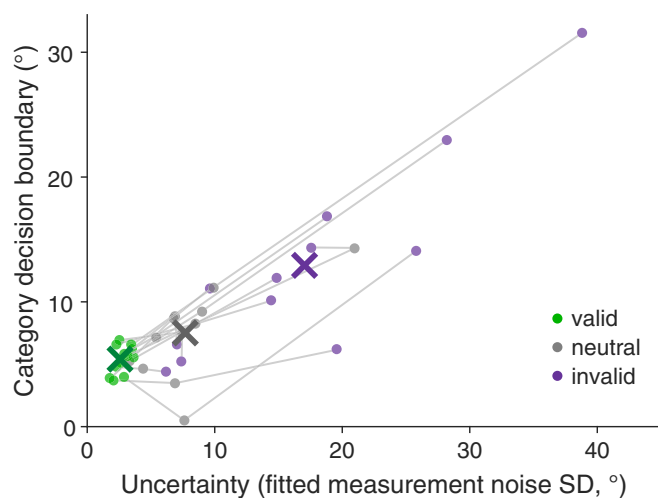


Fig. 4. Free model analysis. Group mean MCMC parameter estimates (crosses) show systematic changes in the category decision boundary across attention conditions. The same pattern can be seen for individual observers: Each gray line corresponds to a different observer, with connected points representing the estimates for valid, neutral, and invalid attention conditions. Each point represents a pair of parameter estimates: uncertainty and category decision boundary for a specific attention condition.

to explain behavioral data from such tasks with a fixed decision rule, as long as the means and variances of the internal measurement distributions are free to vary (*SI Appendix, section S1*).

This issue is particularly thorny for attention studies: SDT works with arbitrary, internal units of “evidence” for one choice or another, and attention could change the means, the variances, or both properties of the internal evidence distributions (10, 11, 36). As a result, the decision boundaries are under-constrained: A fixed decision boundary could be mistaken for a flexible one, and vice versa (Fig. 5). Relatedly, in a perceptual averaging task, confidence data apparently generated by a fixed decision rule can also be explained by a Bayesian decision rule with small underestimations of the internal measurement noise (37). These considerations underscore the importance of doing model comparison even for relatively simple decision models. It may be, then, that decision boundaries did change with attention in previous studies, but these changes were not inferred for methodological reasons.

Alternatively, it may be that decision boundaries truly did not change in previous studies, and task differences underlie our differing results. Studies supporting the unified criterion proposal used either detection or orthogonal discrimination (13, 15, 21–27, 34), which is often used as a proxy for detection (10, 38). In these tasks, the stimuli are low contrast relative to either a blank screen or a noisy background, and performance is limited by low signal-to-noise ratio. In our categorization task, by comparison, although maximum performance is capped due to overlap of the category-conditioned stimulus distributions, variations in performance depend on the precision of orientation representations, just as in a left vs. right fine discrimination task. Therefore, it may be that observers adjust decision boundaries defined with respect to precise features (e.g., What is the exact orientation?) but not boundaries defined with respect to signal strength (e.g., Is anything present at all?).

Other task differences could play a role as well. Some experiments matched perceptual sensitivity d' for different attention conditions by changing stimulus contrast, so attention and physical stimulus properties covaried (13, 15). For the metacognitive report, we asked for confidence rather than visibility (13); these subjective measures are known to differ (39). Finally, one study (15) using a signal detection approach suggested that observers rely insufficiently on an instructed prior, especially for unattended stimuli. The question of how attention affects the use of a prior is different from the current question, as incorporating a prior requires a cognitive step beyond accounting for uncertainty in the perceptual representation. In the future, it will be interesting to examine how decision boundaries relate to priors, attention, and uncertainty more generally in this task and other tasks in which absolute decision boundaries can be uniquely inferred.

Despite attention’s large influence on visual perception (8), only a handful of studies have examined its influence on visual confidence, with mixed results. Two studies found that voluntary attention increased confidence (30, 31), one found that voluntary but not involuntary attention increased confidence (33), and another found no effect of voluntary attention on confidence (32). This last result has been attributed to response speed pressures (30, 33). Three other studies suggested an inverse relation between attention and confidence, though these used rather different attention manipulations and measures. One study reported higher confidence for uncued compared with cued error trials (40), one found higher confidence for stimuli with incongruent compared with congruent flankers (41), and a third found that lower fMRI BOLD activation in the dorsal attention network correlated with higher confidence (21). Here, experimentally manipulating spatial attention without response speed pressure revealed a positive, approximately Bayesian, relation between attention and confidence.

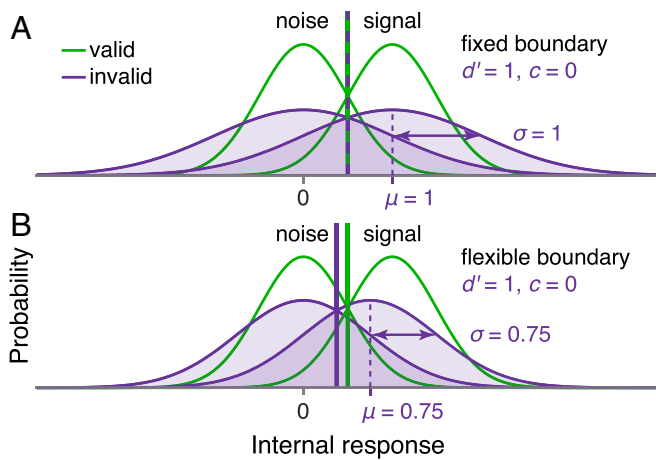


Fig. 5. Limitations of standard SDT tasks. SDT tasks such as the detection task illustrated here cannot distinguish fixed from flexible decision rules when the means and variances of internal measurement distributions can also vary across conditions. (A) Fixed and (B) flexible decision rules give the same behavioral data (perceptual sensitivity, d' , and criterion, c) in the two depicted scenarios, in which attention affects the measurement distributions differently (compare the invalid distributions in A and B). An experimenter could not infer from the behavioral data which scenario occurred.

The mechanisms for decision adjustment under attention-dependent uncertainty could be mediated by effective contrast (10, 42, 43). Alternatively, attention-dependent decision-making may rely on higher order monitoring of attentional state. For example, the observer could consciously adjust a decision depending on whether he or she was paying attention. Future studies will be required to distinguish between these more bottom-up or top-down mechanisms.

Our finding that human observers incorporate attention-dependent uncertainty into perceptual categorization and confidence reports in a statistically appropriate fashion points to the question of what other kinds of internal states can be incorporated into perceptual decision-making. There is no indication, for example, that direct stimulation of sensory cortical areas leads to adjustments of confidence and visibility reports (21, 44, 45), suggesting that the system is not responsive to every change to internal noise. It may be that the system is more responsive to states that are internally generated or that have consistent behavioral relevance. Attention is typically spread unevenly across multiple objects in a visual scene, so the ability to account for attention likely improves perceptual decisions in natural vision. It remains to be seen whether the perceptual decision-making system is responsive to other cognitive or motivational states.

Materials and Methods

Extended materials and methods are available in [SI Appendix](#).

Observers. Twelve observers (seven female) participated in the study. Observers received \$10 per 40- to 60-min session, plus a completion bonus of \$25. The experiments were approved by the University Committee on Activities Involving Human Subjects of New York University. Informed consent was given by each observer before the experiment. All observers were naïve to the purpose of the experiment, and none were experienced psychophysical observers.

Apparatus, Stimuli, and Task. Observers were seated in a dark room, at a viewing distance of 57 cm from the screen, with their head stabilized by a chin-and-head rest. Stimuli were presented on a gamma-corrected 100 Hz, 21-inch display (Model Sony GDM-5402) with a gray background (60 cd/m²). Stimuli were drifting Gabors with spatial frequency of 0.8 cycles per degree of visual angle (dva), speed of 6 cycles per second, Gaussian envelope with SD 0.8 dva, and randomized starting phase. In category training, the stimuli

were positioned at fixation. In all other blocks, one stimulus was positioned in each of the four quadrants of the screen (45, 135, 225, 315°), 5 dva from fixation. On each trial, each of the four stimuli was drawn independently and with equal probability from one of the two category distributions. The main task is shown in Fig. 1 and described in [Results](#). Online eye tracking (Eyelink 1000) was used to ensure fixation.

Experimental Procedure. Each observer completed seven sessions: two staircase sessions (training, contrast staircase, prescreening) followed by five test sessions (main experiment). Observers received instructions and training for each task (see [SI Appendix](#)).

Staircase Sessions. Each staircase session consisted of three category training blocks (72 trials each) and three category/attention testing-with-staircase blocks (144 trials each), in alternation.

In category training blocks, observers learned the stimulus distributions. On each trial, category 1 or 2 was selected with equal probability, the stimulus orientation was drawn from the corresponding stimulus distribution, and the stimulus appeared at fixation for 300 ms at 35% contrast. Observers reported category 1 or 2 and received accuracy feedback after each trial.

In category/attention testing-with-staircase blocks, the trial sequence was identical to the main task (Fig. 1B), except observers reported only category choice. There was no trial-to-trial feedback on this or any other type of attention block.

We used an adaptive staircase procedure (46, 47) to estimate psychometric functions for performance accuracy as a function of contrast, separately for valid, neutral, and invalid trials. Simulations we conducted before starting the study showed that without a sufficiently large accuracy difference between valid and invalid trials, our models would be indistinguishable. Therefore, we used the psychometric function posteriors to determine whether the observer was eligible for the test sessions and, if so, to determine the stimulus contrast for that observer (see [SI Appendix](#)). Twenty-eight observers were prescreened, 13 were invited to participate in the main study, and 1 dropped out, leaving 12 observers, our target.

Test Sessions. Each test session consisted of three category training blocks (identical to staircase sessions but with observer-specific stimulus contrast) and three confidence/attention testing blocks (144 trials each), in alternation. These testing blocks were the main experimental blocks; the trial sequence is shown in Fig. 1B.

Modeling Procedures. The modeling procedures were similar to those used by Adler and Ma (5).

We used free parameters to characterize σ , the SD of orientation measurement noise, for all three attention conditions: σ_{valid} , σ_{neutral} and σ_{invalid} . We added orientation-dependent noise (48).

We coded all responses as $r \in \{1, 2, \dots, 8\}$, with each value indicating category and confidence, as in Fig. 1B. The probability of a single trial i is equal to the probability mass of the internal measurement distribution $p(x | s_i) = \mathcal{N}(x; s_i, \sigma_i^2)$ in a range corresponding to the observer's response r_i . We find the boundaries ($b_{r_i-1}(\sigma_i)$, $b_{r_i}(\sigma_i)$) in measurement space, as defined by the fitting model m and parameters θ , and then compute the probability mass of the measurement distribution between the boundaries:

$$p_{m,\theta}(r_i | s_i, \sigma_i) = \int_{-b_{r_i}}^{-b_{r_i-1}} \mathcal{N}(x; s_i, \sigma_i^2) dx + \int_{b_{r_i-1}}^{b_{r_i}} \mathcal{N}(x; s_i, \sigma_i^2) dx, \quad [1]$$

where $b_0 = 0^\circ$ and $b_8 = \infty^\circ$.

To obtain the log likelihood of the dataset, given a model with parameters θ , we compute the sum of the log probability for every trial i , where t is the total number of trials:

$$\log p(\text{data} | \theta) = \sum_{i=1}^t \log p(r_i | \theta) = \sum_{i=1}^t \log p_\theta(r_i | s_i, \sigma_i). \quad [2]$$

To fit the model, we sampled from the posterior distribution over parameters, $p(\theta | \text{data})$. To sample from the posterior, we use an expression for the log posterior

$$\log p(\theta | \text{data}) = \log p(\text{data} | \theta) + \log p(\theta) + \text{constant}, \quad [3]$$

where $\log p(\text{data} | \theta)$ is given in Eq. 2. We took uniform (or, for parameters that were standard deviations, log-uniform) priors over reasonable, sufficiently large ranges (49), which we chose before fitting any models. We sampled from the probability distribution using a MCMC method, slice sampling (50) (see [SI Appendix](#)).

To compare model fits while accounting for the complexity of each model, we computed the LOO (29). A bootstrapping procedure was used to compute the group mean with CIs for LOO score differences between models.

Bayesian Model. The Bayesian model generates category and confidence responses based on the log posterior ratio, d , of the two categories:

$$d = \log \frac{p(C=1|x)}{p(C=2|x)} = \log \frac{p(x|C=1)}{p(x|C=2)} + \log \frac{p(C=1)}{p(C=2)}. \quad [4]$$

Given the orientation measurement likelihoods, $p(x|C)$, and marginalizing over the stimulus s , this is equivalent to

$$d = \frac{1}{2} \log \frac{\sigma_2^2 + \sigma_1^2}{\sigma_2^2 + \sigma_1^2} - \frac{\sigma_2^2 - \sigma_1^2}{2(\sigma_2^2 + \sigma_1^2)(\sigma_2^2 + \sigma_1^2)} x^2 + \log \frac{p(C=1)}{p(C=2)}. \quad [5]$$

The observer compares d to a set of decision boundaries (k_0, k_1, \dots, k_8), which define the eight possible category and confidence responses. k_4 is the category boundary and captures possible category bias, and it is the only boundary parameter in models of category choice only. k_0 is fixed at $-\infty$ and k_8 is fixed at ∞ , leaving seven free boundary parameters: (k_1, k_2, \dots, k_7) = k .

In the Bayesian models with d noise, we assume that, for each trial, there is an added Gaussian noise term on d , $\eta_d \sim p(\eta_d)$, where $p(\eta_d) = \mathcal{N}(0, \sigma_d^2)$ and σ_d is a free parameter.

- Knill DC, Richards W, eds (1996) *Perception as Bayesian Inference* (Cambridge Univ Press, Cambridge, UK).
- Trommershäuser J, Kording K, Landy MS, eds (2011) *Sensory Cue Integration* (Oxford Univ Press, Oxford).
- Ma WJ, Jazayeri M (2014) Neural coding of uncertainty and probability. *Annu Rev Neurosci* 37:205–220.
- Qamar AT, et al. (2013) Trial-to-trial, uncertainty-based adjustment of decision boundaries in visual categorization. *Proc Natl Acad Sci USA* 110:20332–20337.
- Adler WT, Ma WJ (2018) Comparing Bayesian and non-Bayesian accounts of human confidence reports. bioRxiv:093203. Preprint, posted December 11, 2016.
- Massian P (2016) Visual confidence. *Annu Rev Vis Sci* 2:459–481.
- Fleming SM, Daw ND (2017) Self-evaluation of decision-making: A general Bayesian framework for metacognitive computation. *Psych Rev* 124:91–114.
- Carrasco M (2011) Visual attention: The past 25 years. *Vis Res* 51:1484–1525.
- Reynolds JH, Chelazzi L (2004) Attentional modulation of visual processing. *Annu Rev Neurosci* 27:611–647.
- Carrasco M, Penpeci-Talgar C, Eckstein M (2000) Spatial covert attention increases contrast sensitivity across the CSF: Support for signal enhancement. *Vis Res* 40:1203–1215.
- Lu ZL, Doshier BA (1998) External noise distinguishes attention mechanisms. *Vis Res* 38:1183–1198.
- Anton-Erxleben K, Carrasco M (2013) Attentional enhancement of spatial resolution: Linking behavioural and neurophysiological evidence. *Nat Rev Neurosci* 14:188–200.
- Rahnev D, Maniscalco B, Graves T, Huang E, de Lange FP, Lau H (2011) Attention induces conservative subjective biases in visual perception. *Nat Neurosci* 14:1513–1515.
- Rahnev DA, Bahdo L, de Lange FP, Lau H (2012) Prestimulus hemodynamic activity in dorsal attention network is negatively associated with decision confidence in visual perception. *J Neurophysiol* 108:1529–1536.
- Morales J, et al. (2015) Low attention impairs optimal incorporation of prior knowledge in perceptual decisions. *Atten Percept Psychophys* 77:2021–2036.
- Liu Z, Knill DC, Kersten D (1995) Object classification for human and ideal observers. *Vis Res* 35:549–568.
- Sanborn AN, Griffiths TL, Shiffrin RM (2010) Uncovering mental representations with Markov Chain Monte Carlo. *Cogn Psychol* 60:63–106.
- Geisler WS, Perry JS (2009) Contour statistics in natural images: Grouping across occlusions. *Vis Neurosci* 26:109–121.
- Navajas J, Bahrami B, Latham PE (2016) Post-decisional accounts of biases in confidence. *Curr Op Behav Sci* 11:55–60.
- Cameron EL, Tai JC, Carrasco M (2002) Covert attention affects the psychometric function of contrast sensitivity. *Vis Res* 42:949–967.
- Rahnev DA, Maniscalco B, Luber B, Lau H, Lisansky SH (2012) Direct injection of noise to the visual cortex decreases accuracy but increases decision confidence. *J Neurophysiol* 107:1556–1563.
- Caetta F, Gorea A (2010) Upshifted decision criteria in attentional blink and repetition blindness. *Vis Cognit* 18:413–433.
- Gorea A, Caetta F, Sagi D (2005) Criteria interactions across visual attributes. *Vis Res* 45:2523–2532.
- Zak I, Katkov M, Gorea A, Sagi D (2012) Decision criteria in dual discrimination tasks estimated using external-noise methods. *Atten Percept Psychophys* 74:1042–1055.

Fixed Model. The observer compares the measurement to a set of boundaries that are not dependent on σ . We fit free parameters k and use measurement boundaries $b_r = k_r$.

Linear and Quadratic Models. The observer compares the measurement to a set of boundaries that are linear or quadratic functions of σ . We fit free parameters k and m and use measurement boundaries $b_r(\sigma) = k_r + m_r\sigma$ (Linear) or $b_r(\sigma) = k_r + m_r\sigma^2$ (Quadratic).

Free Model. To estimate the category boundaries with minimal assumptions, we fit free parameters $k_{4, \text{valid}}$, $k_{4, \text{neutral}}$, and $k_{4, \text{invalid}}$ and used measurement boundaries $b_{4, \text{attention condition}} = k_{4, \text{attention condition}}$.

Data and Code Availability. All data and code used for running experiments, model fitting, and plotting are available at <https://doi.org/10.5281/zenodo.1422804>.

ACKNOWLEDGMENTS. The authors thank Roshni Lulla and Gordon C. Bill for assistance with data collection and helpful discussions; Luigi Acerbi for helpful ideas and tools related to model fitting and model comparison; and Stephanie Badde, Michael Landy, and Christopher Summerfield for comments on the manuscript. This material is based upon work supported by the National Science Foundation Graduate Research Fellowship under Award DGE-1342536 (to W.T.A.) and by the National Eye Institute of the National Institutes of Health under Awards T32EY007136 (to New York University) and F32EY025533 (to R.N.D.).

- Gorea A, Sagi D (2000) Failure to handle more than one internal representation in visual detection tasks. *Proc Natl Acad Sci USA* 97:12380–12384.
- Gorea A, Sagi D (2001) Disentangling signal from noise in visual contrast discrimination. *Nat Neurosci* 4:1146–1150.
- Gorea A, Sagi D (2002) Natural extinction: A criterion shift phenomenon. *Vis Cognit* 9:913–936.
- Giordano AM, McElree B, Carrasco M (2009) On the automaticity and flexibility of covert attention: A speed-accuracy trade-off analysis. *J Vis*, 10.1167/9.3.30.
- Veh тари A, Gelman A, Gabry J (2017) Practical Bayesian model evaluation using leave-one-out cross-validation and WAIC. *Stat Comput* 27:1413.
- Zizlsperger L, Sauvigny T, Haarmeier T (2012) Selective attention increases choice certainty in human decision making. *Atten Percept Psychophys* 74:1136–1146.
- Zizlsperger L, Sauvigny T, Händel B, Haarmeier T (2014) Cortical representations of confidence in a visual perceptual decision. *Nat Commun* 5:3940.
- Wilimzig C, Tsuchiya N, Fahle M, Einhäuser W, Koch C (2008) Spatial attention increases performance but not subjective confidence in a discrimination task. *J Vis*, 10.1167/8.5.7.
- Kurtz P, Shapcott KA, Kaiser J, Schmiedt JT, Schmid MC (2017) The influence of endogenous and exogenous spatial attention on decision confidence. *Sci Rep* 7:6431.
- Solovey G, Graney GG, Lau H (2015) A decisional account of subjective inflation of visual perception at the periphery. *Atten Percept Psychophys* 77:258–271.
- Kontsevich LL, Chen C-C, Verghese P, Tyler CW (2002) The unique criterion constraint: A false alarm? *Nat Neurosci* 5:707.
- Doshier BA, Lu ZL (2000) Noise exclusion in spatial attention. *Psych Sci* 11:139–146.
- Zylberberg A, Roelfsema PR, Sigman M (2014) Variance misperception explains illusions of confidence in simple perceptual decisions. *Consc Cognit* 27:246–253.
- Thomas JP, Gille J (1979) Bandwidths of orientation channels in human vision. *J Opt Soc Am* 69:652–660.
- Rausch M, Zehetleitner M (2016) Visibility is not equivalent to confidence in a low contrast orientation discrimination task. *Front Psychol* 7:591.
- Baldassi S, Megna N, Burr DC (2006) Visual clutter causes high-magnitude errors. *PLoS Biol* 4:e56.
- Schoenherr JR, Leth-Steensen C, Petrusic WM (2010) Selective attention and subjective confidence calibration. *Atten Percept Psychophys* 72:353–368.
- Ling S, Carrasco M (2006) Sustained and transient covert attention enhance the signal via different contrast response functions. *Vis Res* 46:1210–1220.
- Carrasco M, Ling S, Read S (2004) Attention alters appearance. *Nat Neurosci* 7:308–313.
- Fetsch CR, Kiani R, Newsome WT, Shadlen MN (2014) Effects of cortical microstimulation on confidence in a perceptual decision. *Neuron* 83:797–804.
- Peters MAK, et al. (2017) Transcranial magnetic stimulation to visual cortex induces suboptimal introspection. *Cortex* 93:119–132.
- Kontsevich LL, Tyler CW (1999) Bayesian adaptive estimation of psychometric slope and threshold. *Vis Res* 39:2729–2737.
- Prins N (2012) The psychometric function: The lapse rate revisited. *J Vis*, 10.1167/12.6.25.
- Girshick AR, Landy MS, Simoncelli EP (2011) Cardinal rules: Visual orientation perception reflects knowledge of environmental statistics. *Nat Neurosci* 14:926–932.
- Acerbi L, Vijayakumar S, Wolpert DM (2014) On the origins of suboptimality in human probabilistic inference. *PLoS Comput Biol* 10:e1003661.
- Neal RM (2003) Slice sampling. *Ann Stat* 31:705–741.

Supplementary Information for
Humans incorporate attention-dependent uncertainty into
perceptual decisions and confidence

Rachel N. Denison^{*1,2}, William T. Adler^{*2}, Marisa Carrasco^{1,2}, Wei Ji Ma^{1,2}

¹Department of Psychology, ²Center for Neural Science,
New York University, New York, NY

Corresponding author:

Rachel Denison
Department of Psychology and Center for Neural Science
New York University
rachel.denison@nyu.edu

This PDF file includes:

Supplementary Text
Extended Materials and Methods
Figures S1–S7
Tables S1–S4
References for SI

* Equal author contribution

Supplementary Text

S1 Theoretical motivations for the task

The goal of the current study was to test whether category and confidence decision rules account for attention-dependent uncertainty. Unlike the tasks used in previous studies, the task we used¹ can answer this question, because it has two properties: 1) Unlike the detection and coarse discrimination (e.g., $\pm 45^\circ$) tasks used in most signal detection theory² (SDT) studies, the current task allows inference of absolute decision boundaries. 2) Unlike tasks with mirror-image categories (e.g., left vs. right discrimination), the current task creates an incentive to shift the category boundary when uncertainty changes.

S1.1 Inference of absolute decision boundaries

A decision rule can be thought of as a boundary defined on the observer’s internal measurement space. Here we were interested in the absolute location of that boundary b . The “unified criterion” discussed previously also refers to an absolute boundary^{3,4}.

To infer absolute decision boundaries from behavioral data, the measurement axis must represent known feature values. The embedded category task has this property, because the measurement axis represents orientation. Making a category or confidence decision can be thought of as comparing the observed stimulus orientation to an internal reference orientation, which is the decision boundary. As experimenters, we know the means of the internal measurement distributions (specific orientations), so we can infer the absolute decision boundary on the orientation axis.

In SDT detection and coarse discrimination tasks, in contrast, absolute decision boundaries cannot be inferred, because the measurement axis represents values that we, as experimenters, do not know. In a detection task, the measurement value is thought of as the strength of the internal signal, or the “amount of evidence” that the external signal is present. In a coarse discrimination task, the measurement value is thought of as the amount of evidence for choice 1 (e.g., -45°) versus choice 2 (e.g., $+45^\circ$). We don’t know the means of the internal measurement distributions in real values; we don’t even know what the units are. Consequently, the behavioral SDT measures d' (perceptual sensitivity) and c (criterion) are defined in a normalized space – d' and c are z-scored measures of the distance between the two internal category distributions and the location of the observer’s decision boundary, respectively. So they are relative measures.

As a result, an absolute decision boundary b is unrecoverable from behavioral data. This fact can be shown mathematically. The standard formulae for d' and c are

$$d' = Z(H) - Z(F) \tag{S1}$$

$$c = -\frac{1}{2}(Z(H) + Z(F)), \tag{S2}$$

where Z is the inverse of the normal cumulative distribution function (i.e., z-score), H is the proportion of hits, and F is the proportion of false alarms. Note this formula gives c with respect to the unbiased criterion. If we let the mean of the noise distribution be 0 and the mean of the signal distribution be μ , then

$$d' = \frac{\mu}{\sigma} \quad (\text{S3})$$

$$c = \frac{b - \frac{\mu}{2}}{\sigma}. \quad (\text{S4})$$

Here we have two equations with three unknowns. Any combination of d' and c is therefore consistent with an infinite set of combinations of the μ , σ , and b parameters; thus b cannot be uniquely determined. The intuition here is that the SDT axis can be rescaled without changing d' and c (**Figure S1a**). The same issue applies not only to d' and c but to any other relative behavioral measure, such as hit rate or false alarm rate. Kontsevich et al.⁵ raised this concern about Gorea and Sagi's⁴ proposal of a unified criterion for simultaneously presented stimuli.

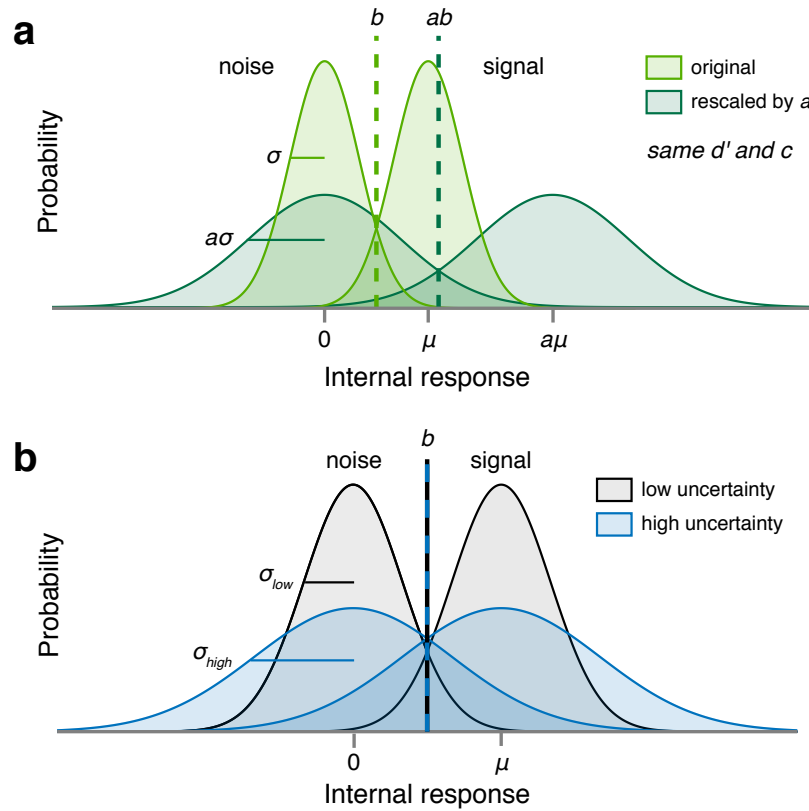


Figure S1: Methodological limitations in standard signal detection tasks. (a) Rescaling the SDT axis by a factor a yields the same values of d' and c , but with a different set of parameters (the original parameters rescaled by a). This is because d' and c are relative to the internal measurement distributions, not any absolute evidence metric. (b) In standard SDT tasks, when the means of the internal measurement distributions are symmetric about the optimal category boundary, changing the uncertainty does not change the optimal boundary. μ = mean, σ = standard deviation, b = decision boundary.

The non-uniqueness of SDT parameters creates a critical problem when asking whether b changes with attention. Attention could change μ , σ , or both properties of the internal measurement distributions⁶⁻⁸. Therefore, b cannot be compared, even in a relative fashion, across attention conditions; so fixed and flexible decision rules cannot be distinguished (**Figure 5**).

Note that in a left vs. right *fine* discrimination task, in which stimuli are drawn from orientation distributions

with similar means, absolute decision boundaries can be inferred, again because the measurement axis represents orientation, and the measurement distribution means are known to the experimenter⁹.

This argument relates to that by Aitchison et al.¹⁰, who showed that to distinguish different models of confidence, two-dimensional data are required. They used features of two separate stimuli. Here, we used orientation and uncertainty.

S1.2 Incentive to shift the category boundary when uncertainty changes

Fine discrimination tasks have the first property, allowing inference of absolute decision boundaries. However, not every such task has the second property, an incentive to shift category boundaries.

In the embedded category task, the category distributions overlap in such a way that the optimal category boundaries shift when the uncertainty in the measurement distributions changes (**Figure 3a,b**). Therefore, observers have an incentive to shift their category decision rules when uncertainty changes, and we as experimenters are able to assess whether they do so.

In standard SDT tasks, in contrast, the optimal category boundary does not depend on uncertainty σ if the means of the internal measurement distributions remain symmetric about the boundary (**Figure S1b**). So if attention does not change the means, or changes them symmetrically (as in a discrimination task), then the optimal category boundary will not change. Observers therefore have no incentive to change their category decision rules when uncertainty changes, making it impossible to test whether the category boundary is fixed or flexible.

In summary, the embedded category task has two critical advantages over standard SDT tasks, which allow an unambiguous determination of whether and how perceptual decisions take uncertainty into account.

Extended Materials and Methods

S2 Experiment

S2.1 Observers

Twelve observers (7 female, 5 male), aged 18–25 years, participated in the experiment. These observers came from an original set of 28 observers who completed at least one session. The remaining observers did not complete the main experiment, either because they were not invited to continue following the pre-screening staircase sessions (15 observers, **Section S2.3.7**) or because they chose to stop participating before all sessions were completed (one observer). Observers received \$10 per 40–60 minute session, plus a completion bonus of \$25. The experiments were approved by the University Committee on Activities Involving Human Subjects of New York University. Informed consent was given by each observer before the experiment. All observers were naïve to the purpose of the experiment. No observers were fellow scientists.

S2.2 Apparatus and stimuli

2.2.1 Apparatus

Observers were seated in a dark room, at a viewing distance of 57 cm from the screen, with their chin in a chinrest. Stimuli were presented on a gamma-corrected 100 Hz, 21-inch display (Model Sony GDM-

5402). The display was connected to a 2010 iMac running OS X 10.6.8 using MATLAB (Mathworks) with Psychophysics Toolbox 3¹¹⁻¹³.

2.2.2 Stimuli

The background was mid-level gray (60 cd/m²). Stimuli consisted of drifting Gabors with a spatial frequency of 0.8 cycles per degree, a speed of 6 cycles/s, a Gaussian envelope with a SD of 0.8 degrees of visual angle (dva), and a randomized starting phase. In category training, the stimuli were positioned at fixation, and the central fixation cross was a black “+” subtending 1.2 dva in diameter. In all other blocks, one stimulus was positioned in each of the four quadrants of the screen, at 45, 135, 225, and 315 degrees, 5 dva from fixation, and the fixation cross was a black “×” with each arm pointing to a quadrant. One or more of the arms turned white to provide a precue or response cue (Figure 1b). Stimulus contrast depended on the block type.

2.2.3 Categories

Stimulus orientations s_i were drawn from Gaussian distributions with means $\mu_1 = \mu_2 = 0^\circ$, and standard deviations $\sigma_1 = 3^\circ$ (category 1) and $\sigma_2 = 12^\circ$ (category 2). Because the category distributions overlapped, maximum accuracy was ~80%.

2.2.4 Attention manipulation

During attention training and testing blocks, voluntary spatial attention was manipulated via a central precue presented at the start of the trial. A response cue at the end of the trial indicated which of the four stimuli to report. On each trial, each of the four stimuli was drawn from one of the two category distributions. Each stimulus was generated independently. In valid trials (66.7% of all trials), a single quadrant was precued and the response cue matched the precue. In invalid trials (16.7%), a single quadrant was precued and the response cue did not match the precue. Cue validity was therefore 80% when a single quadrant was precued. In neutral trials (16.7%), all four quadrants were precued, and the response cue pointed to one of the four quadrants with equal probability for each quadrant.

S2.3 Procedure

Each observer completed seven sessions. Because our behavioral task involved multiple components—orientation categorization, confidence reports, and attention—we trained observers on each component in a stepwise fashion, as described below.

The first two sessions (“staircase sessions”) were used to pre-screen observers and find a stimulus contrast level that would achieve maximum separability in performance across the three attention conditions. Each staircase session consisted of 3 category training blocks and 3 category/attention testing-with-staircase blocks, in alternation. No confidence reports were collected in these sessions. The first category training block was preceded by a category demo, and the first category/attention testing-with-staircase block was preceded by a category/attention training block. Detailed instructions were provided in the first session. Most blocks consisted of sets of trials, in between which the observer was informed of their progress (e.g., “You have completed three quarters of Testing Block 2 of 3”) and allowed to rest. The staircase sessions also served as practice on the categorization and attention components of the task, so that observers knew

them well by the time they started the main experiment. During these sessions, stimulus contrast was 35% for training blocks, and varied during the testing-with-staircase blocks.

The final five sessions (“test sessions”) comprised the main experiment. Each test session consisted of 3 category training blocks and 3 confidence/attention testing blocks, in alternation. The first category training block was preceded by a category demo, and the first confidence/attention testing block was preceded by a confidence/attention training block. During these sessions, stimulus contrast was fixed to an observer-specific value in all blocks.

Combining all test sessions, 9 observers completed 15 confidence/attention testing blocks (2160 trials), 2 observers completed 14 testing blocks (2016 trials), and 1 observer completed 12 testing blocks (1728 trials). Accuracy on category training trials was $70.8\% \pm 4.0\%$ (mean \pm 1 SD) in staircase sessions and $71.9\% \pm 4.0\%$ in test sessions, indicating that observers learned the category distributions well (recall that maximum accuracy on the task is $\sim 80\%$).

2.3.1 Eye tracking

Eye tracking (Eyelink 1000) was used to monitor fixation online. In all blocks, trials were only initiated when the observer was fixating. In testing blocks, trials in which observers broke fixation due to blinks or eye movements were aborted and repeated later in the experiment.

2.3.2 Instructions

First staircase session. Before the first category training block, we provided observers with a printed graphic similar to Figure 1a, explained how the stimuli were generated from distributions, and explained the category training procedure. We also explained that trials would only proceed when the observer maintained fixation. Before the category/attention training block, we explained the attention task using an onscreen graphic that explained the cuing procedure and a printed graphic that illustrated cue validity. We also explained the requirement to maintain fixation from the precue until the response cue and the consequences of breaking fixation. Before the first category/attention testing-with-staircase block, we explained that the stimulus presentation time would be shorter and that the contrast of the stimuli would vary.

First test session. Before the confidence/attention training block, we explained two changes to the experiment. First, we told observers that they would be reporting category choice and confidence simultaneously. We provided a printed graphic similar to the buttons shown in Figure 1b, showing the eight buttons representing category choice and confidence level, the latter on a 4-point scale. The confidence levels were labeled as “very high,” “somewhat high,” “somewhat low,” and “very low.” All printed graphics were visible to observers throughout the experiment. Second, we told observers that contrast would be fixed (rather than variable) for the remainder of the experiment, in all blocks.

2.3.3 Category demo

We showed observers 25 randomly drawn exemplar stimuli from each category (50 exemplars in the first staircase session). Stimulus contrast was 35% in staircase sessions and observer-specific in test sessions.

2.3.4 Category training

To ensure that observers knew the stimulus distributions well, we gave them extensive category training with trial-to-trial correctness feedback and foveal stimulus presentation to reduce orientation uncertainty. Each trial proceeded as follows: Observers fixated on a central cross for 1 s. Category 1 or category 2 was selected with equal probability. The stimulus orientation was drawn from the corresponding stimulus distribution and displayed as a drifting Gabor. The stimulus appeared at fixation for 300 ms, replacing the fixation cross. Observers were asked to report category 1 or category 2 by pressing a button with their left or right index finger, respectively. Observers were able to respond immediately after the offset of the stimulus, at which point correctness feedback was displayed for 1.1 s, e.g., “You said Category 1. Correct!” The fixation cross then reappeared. In staircase sessions, the stimulus contrast was 35%. In test sessions, the contrast matched the observer-specific levels chosen for testing blocks, in order to minimize obvious changes between training and testing blocks. Each category training block had 2 sets of 36 trials (72 total). At the end of the block, observers were shown the percentage of trials that they had correctly categorized.

2.3.5 Category/attention training

To familiarize observers with the attention task before the testing-with-staircase blocks, they completed category/attention training. Observers performed the attention task, reporting only category choice. To prevent observers from forming a simple mapping of orientation measurement and attention condition onto the probability of category 1 (which might have biased behavior towards the Bayesian model), we withheld trial-to-trial feedback on this and all other types of attention blocks. The precue indicating which location(s) to attend to appeared for 300 ms, followed by a 300 ms period in which a standard fixation cross was shown. Then the four drifting Gabor stimuli were displayed for 300 ms. After another 300 ms period with a fixation cross, the response cue appeared, indicating which stimulus to report. The response cue remained on the screen until the observer pressed one of the two choice response buttons, with no time pressure. Observers were free to blink or rest briefly between trials, with a minimum intertrial interval of 800 ms. All attention conditions were randomly intermixed. The stimulus contrast was 35%, as in staircase session category training. The block had 36 trials in the first session and 30 trials in subsequent sessions. At the end of the block, observers were shown the percentage of trials they had correctly categorized.

2.3.6 Category/attention testing-with-staircase

The purpose of this block was to determine the stimulus contrast for each observer that would be used in the test sessions. The trial procedure was identical to that of category/attention training, except that stimulus presentation time was 80 ms (instead of 300 ms) and stimulus contrast varied. We used an adaptive staircase procedure to determine the stimulus contrast on each trial and estimate psychometric functions for performance accuracy as a function of log contrast. Separate staircases were used for valid, neutral, and invalid conditions. We used Luigi Acerbi’s MATLAB (<https://github.com/lacerbi/psybayes>) implementation of the PSI method by Kontsevich and Tyler¹⁴, extended to include the lapse rate¹⁵. The method generates a posterior distribution over three parameters of the psychometric function: threshold μ , slope σ , and lapse rate λ . On each trial, it selects a stimulus intensity that maximizes the expected information gain by completion of the trial. μ (log contrast units) ranged from -6.5 to 0 and had a Gaussian prior distribution with mean -2 and SD 1.2 . $\log \sigma$ ranged from -3 to 0 , and had a uniform prior distribution across the range. λ ranged from 0.15 (because the maximum accuracy in the task was slightly below $1 - 0.15$) to 0.5 , and had a Beta prior distribution with shape parameters $\alpha = 20$ and $\beta = 39$. Each block had 4 sets of 36 trials (144 total). At the end of the block, observers were shown the percentage of trials that they had correctly categorized.

2.3.7 Observer pre-screening and contrast selection

Simulations we conducted before starting the study showed that without a sufficiently large noise (related to accuracy) difference between valid and invalid trials, our models would be indistinguishable. Therefore, we used a pre-screening process to select observers with a robust attention effect to participate in the main experiment. We also determined the stimulus contrast at which each observer’s attention effect was maximal. This procedure increased the probability that uncertainty would depend on attention in the main experiment, which was critical for answering our central question about decision behavior. Note that the pre-screening procedure only concerned the overall accuracy difference between valid and invalid trials, which is independent of how attention affects the decision rule.

After each observer’s final staircase session, we plotted and visually inspected the mean and SD of the posterior over the 3 (valid, neutral, and invalid) estimated psychometric functions (an example is shown in **Figure S7**). An observer was considered eligible for the remainder of the study if there existed a contrast that satisfied two conditions. 1) Invalid accuracy was above chance: The mean minus the SD of the posterior over invalid psychometric functions was above 0.5. 2) Valid accuracy was different from invalid accuracy: The mean minus the SD of the posterior over valid psychometric functions was greater than the mean plus 1 SD of the posterior over invalid psychometric functions. For example, note that there is a range of values in **Figure S7** for which the purple shading does not overlap with the chance line or with the green shading. Within the range of suitable contrasts, we selected the contrast for which the separation between valid, neutral, and invalid performance appeared to be maximal. Observers for which no suitable contrast could be found were not invited to participate in the main experiment. Selected contrasts ranged from 4% to 60% across observers.

2.3.8 Confidence/attention training

To familiarize observers with the button mappings for choice and confidence, they completed confidence/attention training. The trial procedure was identical to category/attention training, except observers reported their confidence on each trial in addition to their category choice. Observers were not instructed to use the full range of confidence reports, as that might have biased them away from reporting what felt most natural. Instead, they were simply asked to be “as accurate as possible in reporting their confidence” on each trial. Feedback about their choice and confidence report was presented for 1.2 s after each trial, e.g. “You said category 2 with HIGH confidence.” The stimulus contrast was specific to each observer, based on the staircase sessions. There were 30 trials per block.

2.3.9 Confidence/attention testing

These were the main experimental blocks. The trial procedure (**Figure 1b**) was the same as in confidence/attention training blocks, but with no trial-to-trial feedback whatsoever. Each block had 4 sets of 36 trials (144 total). At the end of each block, observers were required to take a break of at least 30 s. During the break, they were shown the percentage of trials that they had correctly categorized. Observers were also shown a list of the top 10 block scores (across all observers, indicated by initials). This was intended to motivate observers to perform well, and to reassure them that their scores were normal, since it is rare to score above 75% on a block.

S3 Modeling

The modeling procedures were similar to those used by Adler and Ma⁹. Several modeling choices were adopted based on model comparisons performed for that study. These included: having orientation-dependent measurement noise; allowing all decision boundaries to be free parameters in the Bayesian model; including decision noise in the Bayesian model; and modeling three types of lapse rates.

S3.1 Measurement noise

We used free parameters to characterize σ , the standard deviation (SD) of orientation measurement noise, for all three attention conditions: σ_{valid} , σ_{neutral} , and σ_{invalid} .

We assumed additive orientation-dependent noise in the form of a rectified 2-cycle sinusoid, accounting for the finding that measurement noise is higher at noncardinal orientations¹⁶. For a given trial i , the measurement noise SD comes out to

$$\sigma_i = \sigma_{\text{attention condition}} + \psi \left| \sin \frac{\pi s}{90} \right|. \quad (\text{S5})$$

The second term of this equation is a constant that depends on the stimulus orientation s , with ψ a free parameter that determines the degree of orientation dependence.

S3.2 Response probability

We coded all responses as $r \in \{1, 2, \dots, 8\}$, with each value indicating category and confidence. A value of 1 mapped to high confidence category 1, and a value of 8 mapped to high confidence category 2, as in **Figure 1b**. The probability of a single trial i is equal to the probability mass of the internal measurement distribution $p(x | s_i) = \mathcal{N}(x; s_i, \sigma_i^2)$ in a range corresponding to the observer’s response r_i . Because we only use a small range of orientations, we can safely approximate measurement noise as a normal distribution, rather than a von Mises distribution. We find the boundaries $(b_{r_i-1}(\sigma_i), b_{r_i}(\sigma_i))$ in measurement space, as defined by the fitting model m and parameters θ , and then compute the probability mass of the measurement distribution between the boundaries:

$$p_{m,\theta}(r_i | s_i, \sigma_i) = \int_{-b_{r_i}}^{-b_{r_i-1}} \mathcal{N}(x; s_i, \sigma_i^2) dx + \int_{b_{r_i-1}}^{b_{r_i}} \mathcal{N}(x; s_i, \sigma_i^2) dx, \quad (\text{S6})$$

where $b_0 = 0^\circ$ and $b_8 = \infty^\circ$.

To obtain the log likelihood of the dataset, given a model with parameters θ , we compute the sum of the log probability for every trial i , where t is the total number of trials:

$$\log p(\text{data} | \theta) = \sum_{i=1}^t \log p(r_i | \theta) = \sum_{i=1}^t \log p_{\theta}(r_i | s_i, \sigma_i). \quad (\text{S7})$$

S3.3 Model specification

3.3.1 Bayesian

Derivation of d . The log posterior ratio d is equivalent to the log likelihood ratio plus an additive term representing the prior probability over category:

$$d = \log \frac{p(C = 1 | x)}{p(C = 2 | x)} = \log \frac{p(x | C = 1)}{p(x | C = 2)} + \log \frac{p(C = 1)}{p(C = 2)}. \quad (\text{S8})$$

To get d , we need to find the expressions for the orientation measurement likelihood $p(x | C)$. The observer knows that the measurement x is caused by the stimulus s , but has no knowledge of s . Therefore, the optimal observer marginalizes over s :

$$p(x | C) = \int p(x | s)p(s | C) ds. \quad (\text{S9})$$

We substitute the expressions for the noise distribution and the stimulus distribution, and evaluate the integral:

$$p(x | C) = \int \mathcal{N}(s; x, \sigma^2) \mathcal{N}(s; \mu_C, \sigma_C^2) ds = \mathcal{N}(x; \mu_C, \sigma^2 + \sigma_C^2). \quad (\text{S10})$$

Plugging in the category-specific μ_C and σ_C , and substituting these expressions back into Equation S8, we get:

$$d = \frac{1}{2} \log \frac{\sigma^2 + \sigma_2^2}{\sigma^2 + \sigma_1^2} - \frac{\sigma_2^2 - \sigma_1^2}{2(\sigma^2 + \sigma_1^2)(\sigma^2 + \sigma_2^2)} x^2 + \log \frac{p(C = 1)}{p(C = 2)}. \quad (\text{S11})$$

The 8 possible category and confidence responses are determined by comparing the log posterior ratio d to a set of decision boundaries (k_0, k_1, \dots, k_8) . k_4 is equal to the observer's believed log prior ratio $\log \frac{p(C=1)}{p(C=2)}$, which functions as the boundary between the 4 category 1 responses and the 4 category 2 responses and is fit to capture possible category bias. k_4 is the only boundary parameter in models of category choice only (and not confidence). k_0 is fixed at $-\infty$ and k_8 is fixed at ∞ . The observer chooses category 1 when d is positive. Thus there were 7 free boundary parameters: $(k_1, k_2, \dots, k_7) = \mathbf{k}$.

The posterior probability of category 1 can be written as $p(C = 1 | x) = \frac{1}{1 + \exp(-d)}$.

Decision boundaries. In the Bayesian models with d noise, we assume that, for each trial, there is an added Gaussian noise term on d , $\eta_d \sim p(\eta_d)$, where $p(\eta_d) = \mathcal{N}(0, \sigma_d^2)$, and σ_d is a free parameter. We pre-computed 101 evenly spaced draws of η_d and their corresponding probability densities $p(\eta_d)$. We used Equation S11 to compute a lookup table containing the values of d as a function of x , σ , and η_d . We then used linear interpolation to find sets of measurement boundaries $\mathbf{b}(\sigma)$ corresponding to each draw of η_d ¹⁷. We then computed 101 response probabilities for each trial (as described in **Section S3.2**), one for each draw of η_d , and computed the weighted average according to $p(\eta_d)$. This gave the values of $p_{m,\theta}(r_i | s_i, \sigma_i)$ for each trial i , which are needed in order to compute the total log likelihood of the dataset under the model.

In the Bayesian choice model without d noise, we translate the decision boundary k_4 from a log prior ratio to a measurement boundary corresponding to the fitted noise levels σ . To do this, we use k_4 as the left-hand side of Equation S11 and solve for x at the fitted levels of σ . We used this model only for the purpose of obtaining estimates of the category decision boundary parameters, and not for model comparison.

3.3.2 Fixed

In the Fixed model, the observer compares the measurement to a set of boundaries that are not dependent on σ . We fit free parameters \mathbf{k} and use measurement boundaries $b_r = k_r$.

3.3.3 Linear and Quadratic

In the Linear and Quadratic models, the observer compares the measurement to a set of boundaries that are linear or quadratic functions of σ . We fit parameters \mathbf{k} and \mathbf{m} and use measurement boundaries $b_r(\sigma) = k_r + m_r\sigma$ (Linear) or $b_r(\sigma) = k_r + m_r\sigma^2$ (Quadratic).

3.3.4 Free

To estimate the category boundaries with minimal assumptions, we fit a Free model in which the observer compares the orientation measurement to a set of boundaries that vary nonparametrically (i.e., free of a parametric relationship with σ) across attention conditions. As with the Bayesian choice model without d noise (**Section S3.3.1**), we used this model only for the purpose of obtaining estimates of the category decision boundary parameters and did not fit confidence. We fit free parameters $k_{4,\text{valid}}$, $k_{4,\text{neutral}}$, $k_{4,\text{invalid}}$, and used measurement boundaries $b_{4,\text{attention condition}} = k_{4,\text{attention condition}}$.

S3.4 Lapse rates

In category and confidence models, we fit three different types of lapse rate. On each trial, there is some fitted probability of:

- A “full lapse” in which the category report is random, and confidence report is chosen from a distribution over the four levels defined by λ_1 , the probability of a “very low confidence” response, and λ_4 , the probability of a “very high confidence” response, with linear interpolation for the two intermediate levels.
- A “confidence lapse” $\lambda_{\text{confidence}}$ in which the category report is chosen normally, but the confidence report is chosen from a uniform distribution over the four levels.
- A “repeat lapse” λ_{repeat} in which the category and confidence response is simply repeated from the previous trial.

In category choice models, we fit a standard category lapse rate λ , as well the above “repeat lapse” λ_{repeat} .

S3.5 Parameterization

All parameters that defined the width of a distribution (σ_{valid} , σ_{neutral} , σ_{invalid} , σ_d) were sampled in log-space and exponentiated during the computation of the log likelihood. See **Table S1** for a complete list of model parameters for category choice and confidence models and **Table S3** for choice-only models.

S3.6 Model fitting

Rather than find a maximum likelihood estimate of the parameters, we sampled from the posterior distribution over parameters, $p(\theta \mid \text{data})$; this has the advantage of maintaining a measure of uncertainty about the parameters, which can be used both for model comparison and for plotting model fits. To sample from the posterior, we use an expression for the log posterior

$$\log p(\theta \mid \text{data}) = \log p(\text{data} \mid \theta) + \log p(\theta) + \text{constant}, \tag{S12}$$

where $\log p(\text{data} \mid \theta)$ is given in Equation S7. We assumed a factorized prior over each parameter j :

$$\log p(\theta) = \sum_{j=1}^n \log p(\theta_j), \tag{S13}$$

where j is the parameter index and n is the number of parameters. We took uniform (or, for parameters that were standard deviations, log-uniform) priors over reasonable, sufficiently large ranges¹⁷, which we chose before fitting any models.

We sampled from the probability distribution using a Markov Chain Monte Carlo (MCMC) method, slice sampling¹⁸. For each model and dataset combination, we ran between 4 and 10 parallel chains with random starting points. For each chain, we took 100,000 to 1,000,000 total samples (depending on model computational time) from the posterior distribution over parameters. We discarded the first third of the samples and kept 6,667 of the remaining samples, evenly spaced to reduce autocorrelation. All samples with log posteriors more than 40 below the maximum log posterior were discarded. Marginal probability distributions of the sample log likelihoods were visually checked for convergence across chains. In total we had 120 model and dataset combinations, with a median of 40,002 kept samples (interquartile range = 13,334).

S3.7 Model comparison

3.7.1 Metric choice

To compare model fits while accounting for the complexity of each model, we computed an approximation of leave-one-out cross-validation. Leave-one-out cross-validation is the most thorough way to cross-validate but is very computationally intensive; it requires fitting the model t times, where t is the number of trials. The Pareto smoothed importance sampling approximation of leave-one-out cross-validation (PSIS-LOO, referred to here simply as LOO) takes into account the model’s uncertainty landscape by using samples from the full posterior of θ ¹⁹.

LOO is currently the most accurate approximation of leave-one-out cross-validation²⁰.

We determined that our results were not dependent on our choice of model comparison metric. We computed AIC, BIC, AICc, WAIC²¹, and LOO for all models in the 2 model groupings (category choice-plus-confidence and category choice-only), multiplying the non-LOO metrics by $-\frac{1}{2}$ to match the scale of LOO. For AIC, BIC, and AICc, we selected the MCMC sample with the highest log likelihood as our maximum-likelihood parameter estimate. Then we computed Spearman’s rank correlation coefficient for every possible pairwise comparison of model comparison metrics for all model and dataset combinations, producing 20 total values (2 model groupings \times 10 possible pairwise comparisons of model comparison metrics). All values were greater than 0.998, indicating that, had we used an information criterion instead of LOO, we would not have changed our conclusions. Furthermore, there are no model groupings in which the identities of the lowest- and highest-ranked models are dependent on the choice of metric. The agreement of these metrics strengthens our confidence in our conclusions.

3.7.2 Metric aggregation

In all figures where we present model comparison results (**Figures 3d, S3c, S5b**), we aggregate LOO scores by the following procedure: Choose a reference model (e.g. Fixed). Subtract all LOO scores from the corresponding observer’s score for that model; this converts all scores to a LOO “difference from reference” score, with lower (more negative) indicating a better score and higher (more positive) indicating a worse score. Repeat the following standard bootstrap procedure 10,000 times: Choose randomly, with replacement, a group of datasets equal to the total number of unique datasets, and take the mean of their “difference from reference” scores for each model. Blue lines and shaded regions in model comparison plots indicate the median and 95% CI on the distribution of these bootstrapped mean “difference from reference” scores.

S3.8 Visualization of model fits

Model fits were plotted by bootstrapping synthetic group datasets with the following procedure: For each model and observer, we generated 20 synthetic datasets, each using a different set of parameters sampled, without replacement, from the posterior distribution of parameters. Each synthetic dataset was generated using the same stimuli as the ones presented to the real observer. We randomly selected a number of synthetic datasets equal to the number of observers to create a synthetic group dataset. For each synthetic group dataset, we computed the mean response per orientation bin. We then repeated this 1,000 times and computed the mean and standard deviation of the mean output per bin across all 1,000 synthetic group datasets, which we then plotted as the shaded regions. Therefore, shaded regions represent the mean ± 1 SEM of synthetic group datasets.

For plots with stimulus orientation on the horizontal axis (**Figures 2b, 3c, S3b, S5a**), orientation was binned according to quantiles of the stimulus distributions so that each point consisted of roughly the same number of trials. We took the overall stimulus distribution $p(s) = \frac{1}{2} (p(s | C = 1) + p(s | C = 2))$ and found bin edges such that the probability mass of $p(s)$ was the same in each bin. We then plotted the binned data with linear spacing on the horizontal axis.

S3.9 Model recovery analysis

We performed a model recovery analysis²² to test our ability to distinguish our choice and confidence models. We generated synthetic datasets from each model, using the same sets of stimuli that were originally randomly generated for each of the 12 observers. To ensure that the statistics of the generated responses were similar to those of the observers, we generated responses to these stimuli from 8 of the randomly chosen parameter estimates obtained via MCMC sampling (as described in **Section S3.6**) for each observer and model. In total, we generated 384 datasets (4 generating models \times 12 observers \times 8 datasets). We then fit all four models to every dataset, using maximum likelihood estimation (MLE) of parameters by an interior-point constrained optimization (MATLAB’s *fmincon*), and computed AIC scores from the resulting fits. For reasons of computational tractability, we used AIC instead of LOO as the model comparison metric. Because AIC and LOO scores gave us near-identical model rankings for data from real subjects (**Section S3.7.1**), we do not believe that the model recovery results are dependent on choice of metric.

We found that the true generating model was the best-fitting model, on average, in all cases (**Figure S4**). Overall, AIC “selected” the correct model (i.e., AIC scores were lowest for the model that generated the data) for 87.5% of the datasets, indicating that our models are distinguishable.

Supplementary Figures

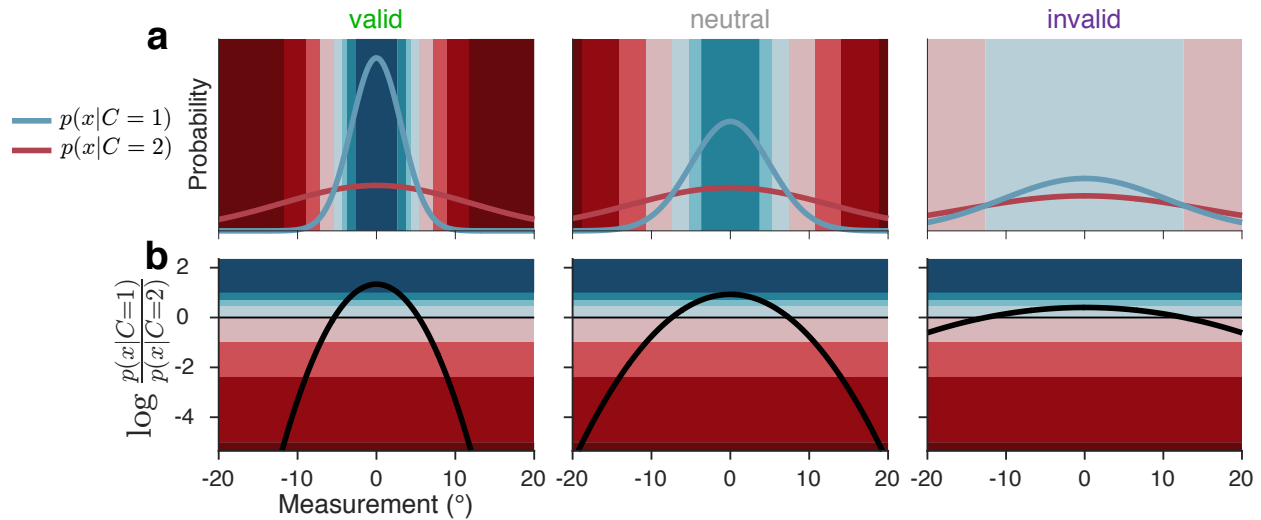


Figure S2: The Bayesian mapping from orientation measurement and attention-dependent uncertainty to response. Colors correspond to category and confidence response as in **Figure 1b**. **(a)** Blue and red curves show likelihood functions for the category distributions under example levels of uncertainty. **(b)** The Bayesian model maps measurement and uncertainty onto the decision variable, the log likelihood ratio (black curve). When the relative likelihood of category 1 is high, the decision variable is large and positive; when the relative likelihood of category 2 is high, it is large and negative. Response is determined by comparing the decision variable to boundaries that are fixed in log-likelihood-ratio space, but in measurement space vary as a function of uncertainty.

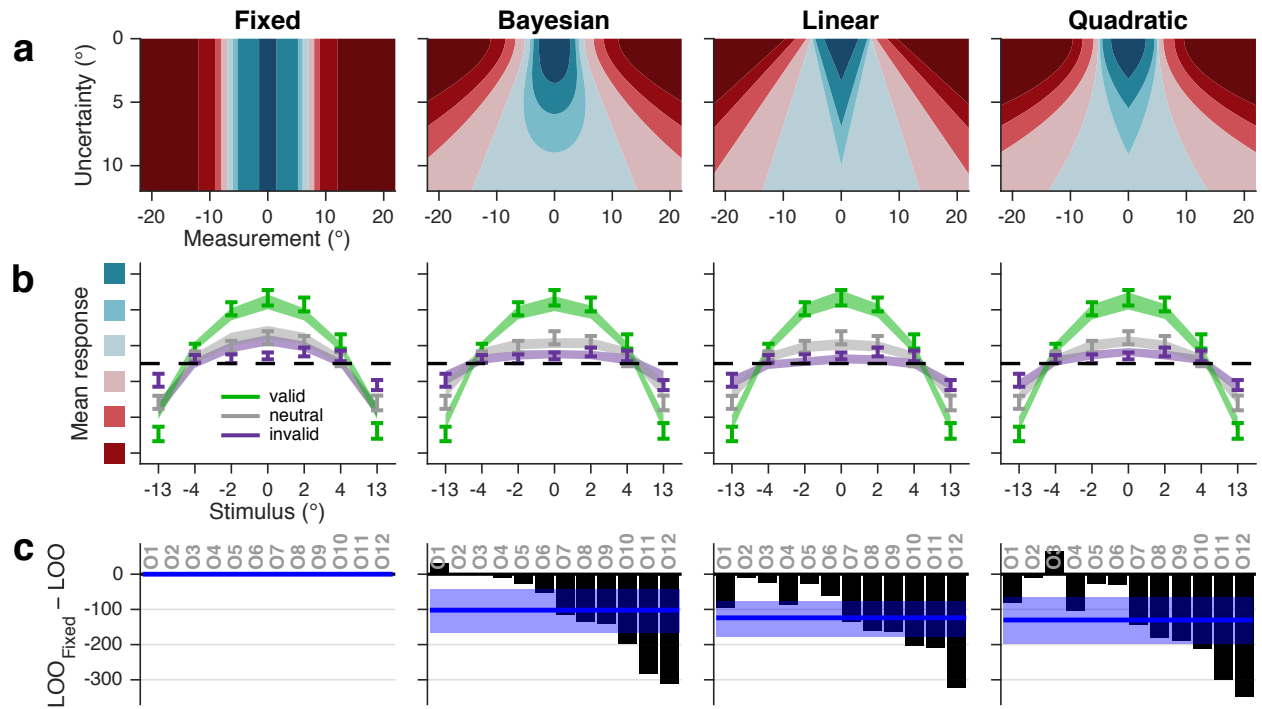


Figure S3: Category and confidence models. (a) Theoretical relation between orientation uncertainty and category and confidence decision boundaries for all models. (b) Mean response as a function of orientation and cue validity, as in **Figure 3c**. Stimulus orientation is binned to approximately equate the number of trials per bin. (c) Model comparison. Black bars represent individual observer LOO score differences of each model from Fixed. Negative values indicate that the corresponding model had a higher (better) LOO score than Fixed. Blue line and shaded region show median and 95% confidence interval of bootstrapped mean LOO differences across observers.

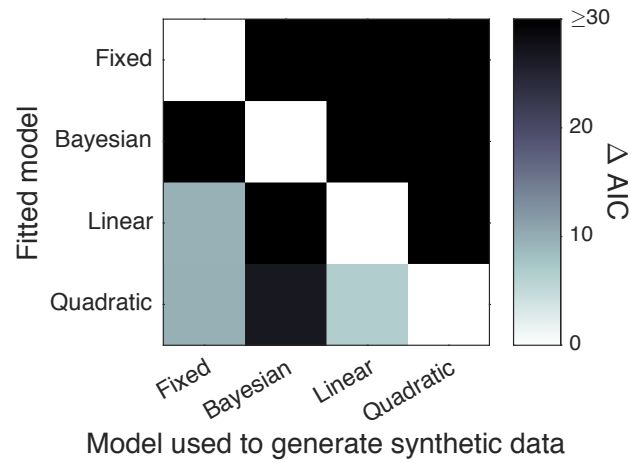


Figure S4: Model recovery analysis. Shade represents the difference between the mean AIC score (across synthetic datasets) for each fitted model and for the one with the lowest mean AIC score. White squares indicate the model that had the lowest mean AIC score when fitted to data generated from each model. The fact that all white squares lie on the diagonal indicates that the true generating model was the best-fitting model, on average, in all cases.

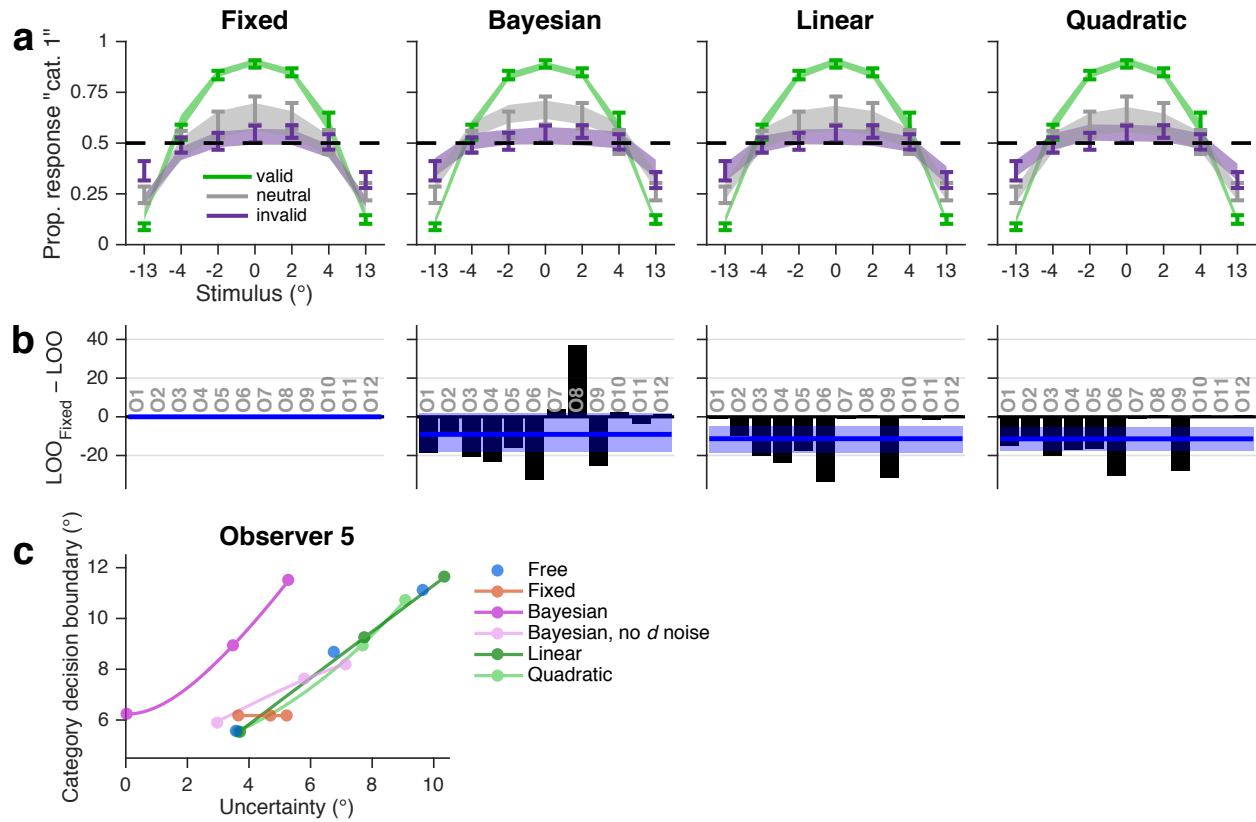


Figure S5: Category choice-only models. (a) Proportion of category 1 responses as a function of orientation and cue validity. Error bars show mean and SEM across observers. Shaded regions are mean and SEM of model fits (Section S3.8). Stimulus orientation is binned to approximately equate the number of trials per bin. (b) LOO model comparison, as in Figure S3c. (c) Mean MCMC orientation uncertainty and category choice boundary parameter estimates for a representative observer. Estimates are plotted as a function of attention condition (valid, neutral, invalid; filled circles), along with their generating functions (curves), for the four main models fit to the category choice data only, plus a Bayesian model with no noise on the decision variable d and a nonparametric model in which choice boundaries are unconstrained (Free; parameter estimates from this model are plotted in gray for all subjects in Figure 4). The Bayesian curve is to the left of the other curves, because noise attributed to orientation uncertainty in the other models is partially attributed to decision noise in the Bayesian model; when the decision noise parameter is removed (Bayesian, no d noise), the curve aligns with the others.

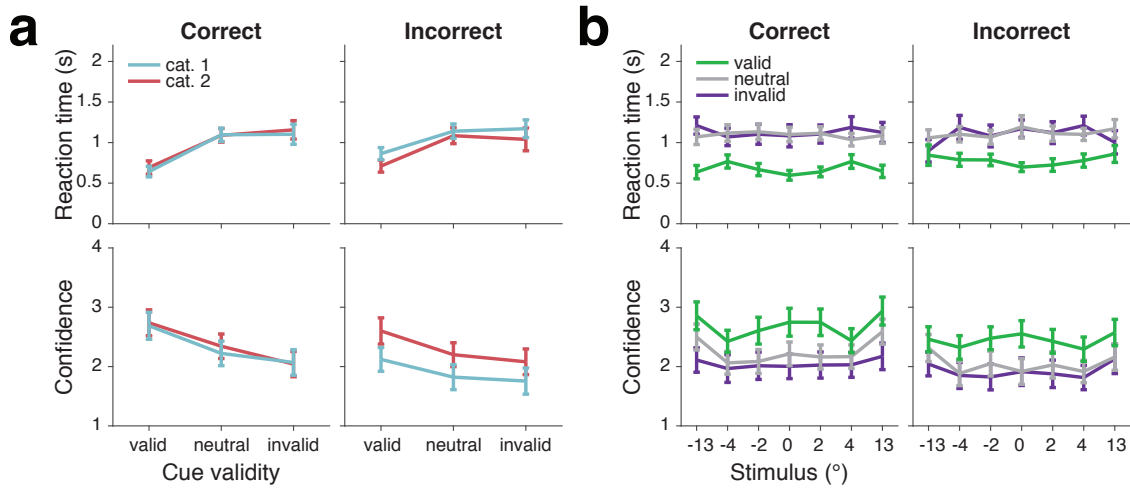


Figure S6: RT and confidence data broken down by category and accuracy. RT did not depend strongly on category or accuracy, though it was slightly longer for valid incorrect compared to valid correct trials. Confidence was higher overall for correct compared to incorrect trials. Confidence was higher and RT slightly faster for category 2 incorrect trials compared to category 1 incorrect trials, likely because there are more category 2 trials with high probability of being category 1 (which would lead to a high confidence error) than category 1 trials with high probability of being category 2.

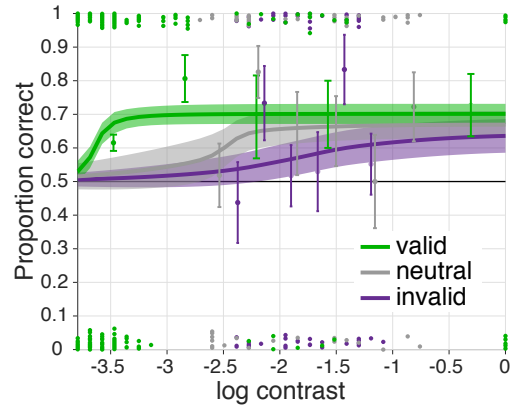


Figure S7: Example plot used to determine per-observer stimulus contrast. Each curve shows the mean ± 1 SD of the posterior over psychometric functions for each attention condition. Error bars indicate the mean ± 1 SD of the beta distribution over correctness within log contrast bins. A dot indicates one correct or incorrect trial, located respectively at the top or bottom of the plot, with vertical jitter. For this example observer, we selected a natural log contrast of -2.3 (i.e., a contrast of 10%).

Supplementary Tables

	Fixed	Bayesian	Linear	Quadratic
Measurement noise	$\sigma_{\text{valid}}, \sigma_{\text{neutral}}, \sigma_{\text{invalid}}$			
Orientation-dependent noise	ψ			
Decision boundaries	k_{1-7}		k_{1-7}, m_{1-7}	
d noise	σ_d			
Lapse rates	$\lambda_1, \lambda_4, \lambda_{\text{confidence}}, \lambda_{\text{repeat}}$			
Total number of parameters	15	16	22	22

Table S1: Parameters of category choice and confidence decision models.

	15 pars. Fixed	16 pars. Bayesian	22 pars. Linear
22 pars. Quadratic	129 [65, 198]	27 [0, 53]	5 [-18, 28]
22 pars. Linear	124 [77, 177]	21 [-3, 48]	
16 pars. Bayesian	102 [45, 167]		

Table S2: Cross comparison of all category choice and confidence decision models. Cells indicate medians and 95% CI of bootstrapped mean LOO score differences. A positive median indicates that the model in the corresponding row had a higher score (better fit) than the model in the corresponding column.

	Fixed	Bayesian	Bayesian, no d noise*	Linear	Quadratic	Free*
Measurement noise	$\sigma_{\text{valid}}, \sigma_{\text{neutral}}, \sigma_{\text{invalid}}$					
Orientation-dependent noise	ψ					
Decision boundaries	k			k, m		$k_{\text{valid}}, k_{\text{neutral}}, k_{\text{invalid}}$
d noise	σ_d					
Lapse rates	$\lambda, \lambda_{\text{repeat}}$					
Total number of parameters	7	8	7	8	8	9

Table S3: Parameters of category choice-only decision models. * indicates models that were used only for obtaining parameter estimates (**Figures 4, S5c**), and not for model comparison.

	7 pars. Fixed	8 pars. Bayesian	8 pars. Linear
8 pars. Quadratic	11 [5, 18]	2 [-2, 9]	0 [-2, 3]
8 pars. Linear	11 [4, 19]	2 [-3, 10]	
8 pars. Bayesian	9 [-2, 18]		

Table S4: Cross comparison of all category choice-only decision models. Conventions as in **Table S2**.

References

- [1] Qamar, A. T. *et al.* Trial-to-trial, uncertainty-based adjustment of decision boundaries in visual categorization. *Proc Nat Acad Sci USA* **110**, 20332–20337 (2013).
- [2] Green, D. M. & Swets, J. A. *Signal detection theory and psychophysics* (Wiley, New York, 1966).
- [3] Gorea, A. & Sagi, D. Failure to handle more than one internal representation in visual detection tasks. *Proc Natl Acad Sci USA* **97**, 12380–12384 (2000).
- [4] Gorea, A. & Sagi, D. Disentangling signal from noise in visual contrast discrimination. *Nat Neurosci* **4**, 1146–1150 (2001).
- [5] Kontsevich, L. L., Chen, C.-C., Verghese, P. & Tyler, C. W. The unique criterion constraint: a false alarm? *Nat Neurosci* **5**, 707 (2002).
- [6] Lu, Z. L. & Doshier, B. A. External noise distinguishes attention mechanisms. *Vis Res* **38**, 1183–1198 (1998).
- [7] Carrasco, M., Penpeci-Talgar, C. & Eckstein, M. Spatial covert attention increases contrast sensitivity across the CSF: support for signal enhancement. *Vis Res* **40**, 1203–1215 (2000).
- [8] Doshier, B. A. & Lu, Z. L. Noise exclusion in spatial attention. *Psych Sci* **11**, 139–146 (2000).
- [9] Adler, W. T. & Ma, W. J. Comparing Bayesian and non-Bayesian accounts of human confidence reports. *bioRxiv* 093203 (2018). [related:qMQe6XVts8AJ](#).
- [10] Aitchison, L., Bang, D., Bahrami, B. & Latham, P. E. Doubly Bayesian analysis of confidence in perceptual decision-making. *PLoS Comput Biol* **11**, e1004519 (2015).
- [11] Pelli, D. G. The VideoToolbox software for visual psychophysics: transforming numbers into movies. *Spat Vis* **10**, 437–442 (1997).
- [12] Brainard, D. H. The Psychophysics Toolbox. *Spat Vis* **10**, 433–436 (1997).
- [13] Kleiner, M., Brainard, D. H. & Pelli, D. G. What’s new in Psychtoolbox-3? ECVP Abstract Supplement . *Perception* **36** (2007).
- [14] Kontsevich, L. L. & Tyler, C. W. Bayesian adaptive estimation of psychometric slope and threshold. *Vis Res* **39**, 2729–2737 (1999).
- [15] Prins, N. The psychometric function: the lapse rate revisited. *JOV* **12**, 25–25 (2012).
- [16] Girshick, A. R., Landy, M. S. & Simoncelli, E. P. Cardinal rules: Visual orientation perception reflects knowledge of environmental statistics. *Nat Neurosci* **14**, 926–932 (2011).
- [17] Acerbi, L., Vijayakumar, S. & Wolpert, D. M. On the origins of suboptimality in human probabilistic inference. *PLoS Comput Biol* **10**, e1003661 (2014).
- [18] Neal, R. M. Slice sampling. *Ann Stat* **31**, 705–741 (2003).
- [19] Vehtari, A., Gelman, A. & Gabry, J. Efficient implementation of leave-one-out cross-validation and WAIC for evaluating fitted Bayesian models. *arXiv* 1507.04544v1 (2015). [3706900867636205788related:3BgL-bK0cTMJ](#).
- [20] Acerbi, L., Dokka, K., Angelaki, D. E. & Ma, W. J. Bayesian comparison of explicit and implicit causal inference strategies in multisensory heading perception. *bioRxiv* e150052 (2017).

- [21] Gelman, A., Hwang, J. & Vehtari, A. Understanding predictive information criteria for Bayesian models. *Stat Comput* **24**, 997–1016 (2014).
- [22] van den Berg, R., Awh, E. & Ma, W. J. Factorial comparison of working memory models. *Psych Rev* **121**, 124–149 (2014).